NANOSIZE RADIATION DEFECTS in ARSENIC IMPLANTED HgCdTe EPITAXIAL FILMS of n- and p-TYPE STUDIED with TEM/HRTEM

Ihor I. Izhnin[1] (i.izhnin@carat.electron.ua), K.D. Mynbaev[2], Z. Swiatek[3], J. Morgiel[3], A.V. Voitsekhovskii[4], A.G. Korotaev[4], O.I. Fitsych[5], V.S. Varavin[6], S.A. Dvoretsky[6], N.N. Mikhailov[6], M.V. Yakushev[6], O.Yu. Bonchyk[7], H.V. Savytskyy[7]

[1] Scientific Research Company "Electron-Carat", Lviv, Ukraine
[2] Ioffe Institute, Saint- Petersburg, Russia
[3] Institute of Metallurgy and Material Science PAN, Krakow, Poland
[4] National Research Tomsk State University, Tomsk, Russia
[5] P. Sagaidachny Army Academy, Lviv, Ukraine
[6] A.V. Rzhanov Institute of Semiconductor Physics, SB RAS, Novosibirsk, Russia
Ya.S. Pidstryhach Institute for Applied Problems of Mechanics and Mathematics NASU, Lviv, Ukraine

INTRODUCTION

- For $Cd_xHg_{1-x}Te$ (MCT), the basic material for infrared photo–electronics, there are various configurations of *p-n* junctions of photodiodes; for their creation, ion implantation is usually used.
- The most promising design of *p–n* junctions used in photodiodes based on MCT, relies on fabrication of local *p*–type regions in an *n*–type base with the use of implantation of arsenic.
- Ion implantation, however, leads to the formation of various types of radiation donor defects, so to form a required *p*–type region one needs to anneal the radiation defects and to activate the introduced arsenic atoms electrically.
- To perform an effective annealing, it is necessary to know the properties and nature of the radiation donor defects. However, the effect of the arsenic implantation on the properties of MCT is typically studied after implantation into *p*–type material. This approach presumes that formation of implantation-induced defects, including electrically active ones, proceeds similarly in the 'base' layers with *p*– and *n*–type conductivity.
- To the best of our knowledge, no direct proof to this fact has been given yet with the exception of very limited data obtained with single-field Hall-effect measurements on MCT epitaxial films implanted with nitrogen.
- **The aim of this work was to performed a direct comparison with TEM/HRTEM of the effect of arsenic implantation on the properties of *n*– and *p*–type samples made from the same epitaxial $Hg_{0.78}Cd_{0.22}Te$ film, – in relation to their radiation defects type, structure, size.**

BF-TEM images

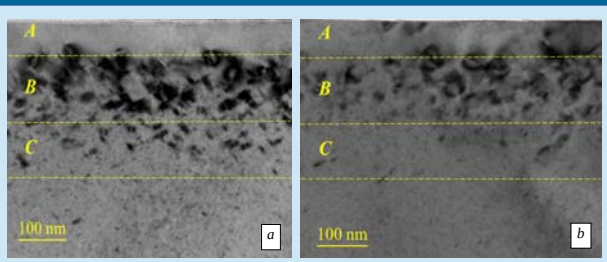

Fig.1. BF-TEM images of the cross-sectional views of samples #1 (n-type, a) and #2 (p-type, b). The material was implanted with As at E=190 keV and Φ=10¹⁴ cm⁻².

Whole implantation-damaged layer (Fig. 1) for both samples extended to a considerable depth, almost to 330 nm. The layer could be divided into three characteristic sub-layers. The top sub-layers *A* had thicknesses ~70 nm in both samples and possessed a low density of structural defects. Sub-layers *A* were followed by sub-layers *B*, which contained 'large' structural defects with high densities. The thicknesses of the sub-layers *B* equaled ~120 nm in both samples. Sub-layers *C*, which contained 'small' extended defects with lower densities. These sub-layers were followed by the layers containing quasi-point defects, which could not be visualized in BF-TEM mode and appeared as a uniform background.

In sub-layer *A* for sample #1 and #2 (Fig. 2) one can observe isolated small vacancy-type dislocation loops (3 = 5 nm) in size against the background of almost perfect crystalline structure. A stacking fault and some single dislocations are seen in the image.

Sub-layer *B* for sample #1 and #2 (Fig. 3) contains high density of large extended structural defects - dislocation loops with various sizes (10-30 nm), single dislocations, a stacking faults. In fact, these loops are the dominating defects in this layer.

The defects in the sub-layer *C* were smaller in size and concentration than those in the sub-layer *B* (not presented). In general, the defect patterns formed by the implantation in MCT with *p*–type conductivity and *n*–type conductivity appeared to be very similar.

HRTEM radiation defects images

EXPERIMENTAL DETAILS

❑ In-doped film was grown by molecular-beam epitaxy at Institute of Semiconductor Physics (Novosibirsk) on (013) CdTe/ZnTe/Si substrates; *in situ* ellipsometric measurements were used to monitor their composition and thickness. Their 'absorber' layer with uniform CdTe molar fraction (composition) x_0~0.22 was covered with a graded-gap protective layer (GPL) with composition at the surface x_s=0.46. The thickness of the GPL was ~0.4 μm.

❑ Indium doping provided *n*-type conductivity of the as-grown film (n=4·10¹⁵ cm⁻³). A piece cut from the film after the growth was subjected to thermal annealing (220 °C, 24 h) in helium atmosphere at low mercury pressure. As a result of the annealing, a *p*–type sample was fabricated with hole conductivity resulting from the presence of mercury vacancies, intrinsic acceptors in MCT (p=5.1·10¹⁵ cm⁻³).

❑ Both *n*– (#1) and *p*–(#2) type samples were implanted in one implantation cycle with As^+ ions with the energy 190 keV and fluence 10^{14} cm⁻² using IMC200 (Ion Beam Services, France) machine. The microstructure of the implanted material was studied with Transmission Electron Microscopy (TEM) in bright-field (BF) and high-resolution (HRTEM) modes with the use of Tecnai G2 F20, FEI Company microscope. Thin foils were prepared using FEI Quanta 200 dual-beam focused-ion (Ga+) beam machine equipped with an OmniprobeTM lift-out system.

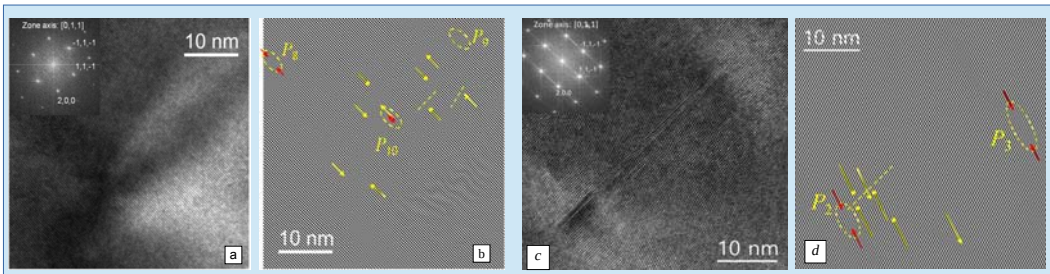

Fig. 2. HRTEM image of an area in the sub-layer A of sample #1 (a. b, n-type) and sample #2 (c, d, p-type). Inset showing its fast Fourier transform (FFT) image (a, c), and corresponding inverse FFT (IFFT) image (b, d). Red arrows and dashed ovals in image (b, d) mark dislocation loops; yellow arrows, single dislocations, dashed line a stacking fault. .

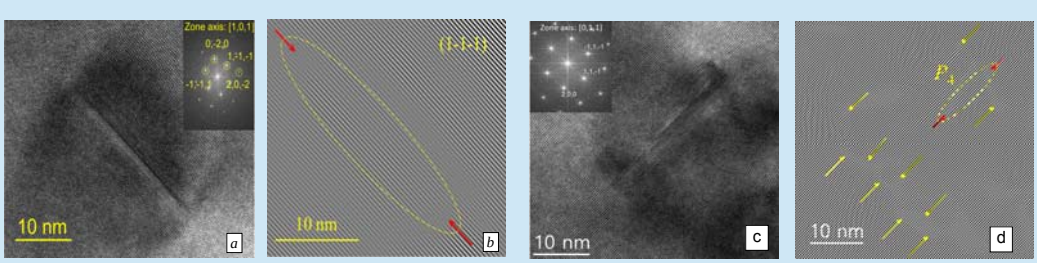

Fig. 3. HRTEM image of an area in the sub-layer B of sample #1 (a, b, n-type) and sample #2 (c, d, p-type). Inset showing its fast Fourier transform (FFT) image (a, c), and corresponding inverse FFT (IFFT) image (b, d). Red arrows and dashed ovals in image (b, d) mark dislocation loops, yellow arrows single dislocations.

Conclusions

❑In general the effect of the As implantation on the structural quality of the surface appeared to be very similar in *n*– and *p*–type material.

❑ BF–TEM studies showed that the defect layers produced by the As implantation were similar in *n*– and *p*–type samples in terms of the thicknesses of the damaged layers. The layer could be divided into three characteristic sub-layers. The top sub-layers *A* had thicknesses ~70 nm in both samples and possessed a low density of structural defects. Sub-layers *A* were followed by sub-layers *B*, which contained 'large' structural defects with high densities. The thicknesses of the sub-layers *B* equaled ~120 nm in both samples. The sub-layers *B* were followed by ~100 nm-thick sub-layers *C*, which contained 'small' extended defects with lower densities.

❑ HRTEM studies showed that the defect layers produced by the As implantation were also similar in *n*– and *p*–type samples in terms of the types and size of the induced defects. The sub-layers *A* contains isolated dislocation loops of small size, stacking fault and some single dislocations against the background of almost perfect crystalline structure. The sub-layer *B* contained high density of large extended structural defects along with defect complexes and agglomerates. In fact, these dislocation loops are the dominating defects in this layer. The defects in the sub-layer *C* were smaller in size and density than those in the sub-layer *B*.